This is an Accepted Manuscript of an article published by Taylor & Francis in Molecular Simulation on 2019-12-12, available online: https://www.tandfonline.com/10.1080/08927022.2019.1660326.

Structural Properties of sH Hydrate: A DFT Study of Anisotropy and Equation of State

Authors: Shaden M. Daghash[a], Phillip Servio[a], Alejandro D. Rey[a]*

[a] *Department of Chemical Engineering, McGill University, Montréal, Quebec H3A 0C5, Canada*

*Corresponding author email: alejandro.rey@mcgill.ca

Structural Properties of sH Hydrate: A DFT Study of Anisotropy and Equation of State

Abstract

Structure-H (sH) hydrate is one of the canonical gas hydrates with significant potential applications and scarce characterized material properties despite the wide knowledge available on other gas hydrates. In this work we characterize some of the important physical properties of this hydrate at the atomistic level using Density Functional Theory. Two exchange-correlation functionals (revPBE and DRSLL) were used to simulate six sH hydrate systems encapsulating neohexane and different help gas molecules. The important role of dispersion forces is quantified. The density and isothermal bulk modulus of sH hydrate are higher when dispersion interactions are considered. The presence of those interactions imposes a direct relationship between the hydrate density and its bulk modulus, while their absence reveals the bulk modulus dependency on hydrogen bond density. Anisotropy is a distinguishing feature of this hydrate in distinction to nearly isotropic sI and sII hydrates. Structure-H hydrate experiences a compressional anisotropy in which the a-lattice and the c-lattice constants respond differently to applied pressure showing less compressibility along the c-axis. This compressional anisotropy was found dependant on the chemistry of help gas molecules. Taken together, these property characterization results and analysis are a significant and novel contribution to the material physics of sH hydrates.

Keywords

Density Functional Theory, sH hydrate, compressional anisotropy, isothermal bulk modulus, hydrogen bond density

Introduction

Gas hydrates represent a type of clathrates that have a structure made by hydrogen-bonded water molecules forming cages of different sizes and encapsulating different types of guest molecules [1, 2]. They are non-stoichiometric inclusion compounds that don't need a full occupancy of their cages to stabilize [3]. They can be synthesized and are found to naturally occur in the seafloor sediments encapsulating mainly methane gas. Since their discovery in 1800 [4], gas hydrates became the scope of work of many researchers, and later in 1934 they attracted industrial interest by causing gas pipeline blocking problems [5, 6]. Emerging gas hydrates applications include energy materials, and CO_2 capture [7, 8]. However, their natural existence as reserves for natural gas makes them an energy source and a geohazard at the same time. The environmental impacts of gas hydrates dissociation and extraction have become a concern due to their contribution to potential climate problems and the instability of seafloor geology [9].

The three main types of gas hydrates are the cubic sI and sII structures consisting of two cage sizes, and the hexagonal sH hydrate. sH hydrate is distinguishable by having three different types of cages and being a binary hydrate that needs two guest's molecules sizes to form and stabilize, a large gas molecule substance (LGMS) and a small (help gas) one. The large cages have the ability to encapsulate large size molecules of diameter size of 7.5-8.6 Å [10], such as neohexane, methylcyclohexane, pinacolone, t-butyl methyl ether [4], and water soluble hexamethyleneimine [11]. It was found to form at pressures lower than the formation pressure of sI hydrate [12]. sH hydrate was first discovered by Ripmeester [4] in 1987 and was found naturally in the Gulf of Mexico slope's [13]. Its crystal structure belongs to the P6/mmm space group [14]. One-unit cell of sH hydrate consists of 34 water molecules forming three sizes of cages, three small 5^{12} pentagonal dodecahedron cages, two medium $4^3 5^6 6^3$ irregular

dodecahedron cages, and one $5^{12}6^8$ icosahedron cage forming a hexagonal unit cell [14]. Structure-H hydrate has been identified by its structure anisotropy [15, 16, 17] and the dependency of its properties on directionality.

Characterizing and understanding the mechanical properties of gas hydrates is critical for the proper exploitation of gas hydrates as well as the inhibition of their geological hazards [18]. There are a few experimental and simulation-based studies that investigated the properties of sH hydrate [13, 15, 19, 20, 21, 22]. Some researchers explored the factors affecting the stability of sH hydrate [14, 19, 23, 24], while others focused on sH structural anisotropy [15, 19]. Imasato *et al.* [22] studied the effect of LGMS molecular volume on sH hydrate lattice constants. Murayama *et al.* [15] inspected the effect of help gas molecule size on the properties of neohexane sH hydrate. The formation kinetics of sH hydrate was reviewed and found dependent of the type of LGMS [25, 26]. First principle computations were used to study sH hydrate properties [9, 20, 27, 28, 29, 30]. However, a complete set of properties of sH hydrate is not yet available, and although ice properties have been used to approximate hydrate behavior [31], this method proved its inadequacy due to the significant differences between them [27]. Understanding sH hydrate structure and its physical properties is of great interest due to its high methane storage capacity compared to sI and sII hydrates [21, 32], its low formation pressure [12], and its stabilization conditions [33].

The present work involves ab-initio atomistic level simulations at 0 K to understand some of the mechanical properties of sH hydrate using Density Functional Theory (DFT). DFT computations aim to better understand the discrepancy of experimental results by compensation with information that are not experimentally biased [34]. All simulations are done using two exchange-correlation (XC) functionals, the semi-local GGA-revPBE and the non-local vdW-

DRSLL to emphasize the importance of guest-host van der Waal interactions in defining sH hydrate structure and properties. The objectives and scope of this work is to understand the compressional behaviour of different sH hydrate systems including the empty metastable hydrate structure. The isothermal equation of state (EOS) fitting using different equations is done to estimate the hydrate incompressibility and how the lattice structure changes with pressure, the hydrate density, the hydrogen-bond density, and type of help gas. The structural anisotropy of sH hydrate is also examined and a comprehensive comparison of this hydrate type to sI, sII, and ice (Ih) under the above-mentioned load conditions is provided.

The organization of this paper is as follows. Section II includes a description of the DFT computational methods implemented in this work, the exchange-correlation functional selection, and the isothermal EOS fitting. The analysis and discussion of results are presented in section III with comparison of findings to other hydrate structures and ice (Ih). Section IV presents the conclusion and key outcomes of this work.

Computational Methods

sH hydrate consists of multi-unit cells that are hexagonal in structure. As mentioned above, the unit cell has 34 water molecules that form three types of cages, one large $5^{12}6^{8}$ cage, two medium $4^{3}5^{6}6^{3}$ cages, and three small 5^{12} cages. A unit cell of methane and neohexane (NH) sH hydrate is presented in Figure 1.

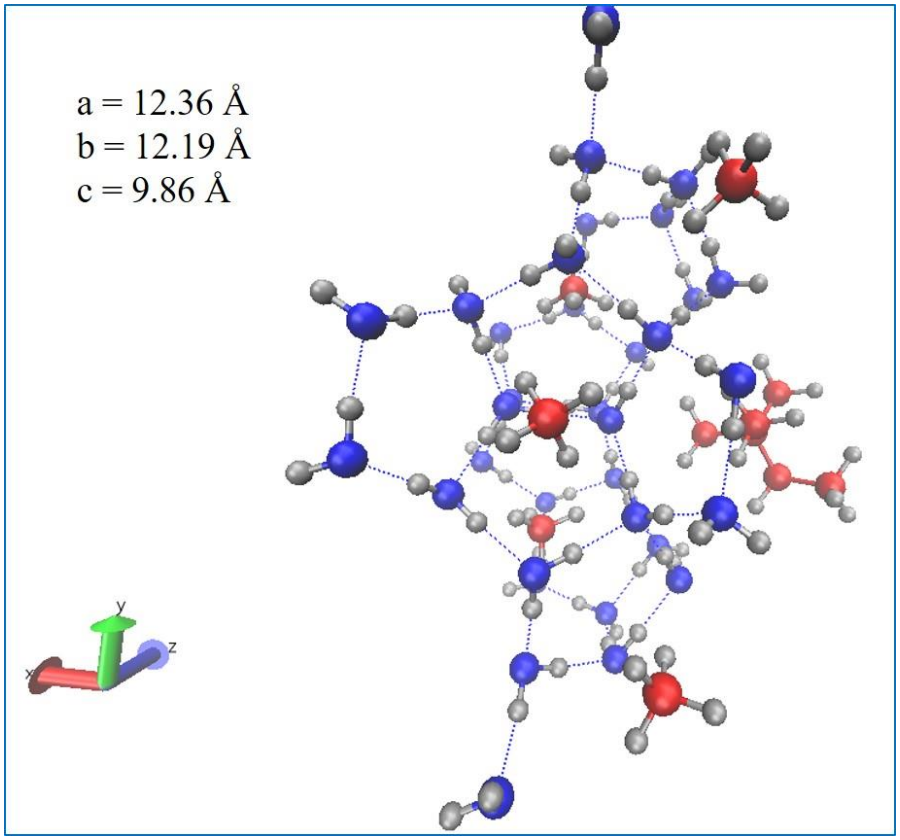

Figure 1: A unit cell of sH hydrate encapsulating methane and neohexane (NH) visualized by VMD [35].

The small cage structure is the same as that of sI and sII hydrates, however, the medium and large cages are unique geometry blocks of the sH hydrate. This type of hydrate requires two different sizes of guests to form and stabilize. A LGMS encapsulated inside the large cage and a small guest (help gas) that occupies the small and medium cages. Studying structures at the atomistic level is critical in understanding the physical properties of materials. One-unit cell of sH hydrate is used in performing Density Functional Theory (DFT) simulations at 0 K due to the highly demanding computational cost of DFT simulations.

DFT simulations were done using the Spanish Initiative for Electronic Simulations with Thousands of Atoms (SIESTA) [36] software. The total system energy in DFT simulations are minimized by solving the Kohn-Sham equations. SIESTA generates a supercell consisting of

eight-unit cells with periodic boundary conditions. Two different types of exchange-correlation (XC) functionals were used to evaluate the effect and intensity of guest-host interactions on the mechanical properties of sH hydrate. The revised Perdew−Burke−Ernzer- hof (revPBE) [37] Generalized Gradient Approximation (GGA) functional proved its effectiveness in DFT simulation studies related to gas hydrates [31, 38]. However, as this functional doesn't account for the dispersion interactions between guest molecules and host cages, another functional was used for comparison. Different van der Waal functionals in SIESTA were tested and vdW-DRSLL was selected. DRSLL is a van der Waal functional of Dion *et al*. [39] with the implementation of Román-Pérez and Soler [40].

The initial structure of the empty sH hydrate was obtained from data in Okano and Yasuoka [41]. The hydrogen atoms were placed in an arrangement that abides by the ice rules and generates a unit cell with zero dipole moment. The selected structure as most suitable is the one with the lowest potential energy and dipole moment [41]. The guest molecules were generated and placed at the centre of cages with a single molecule occupancy in each cage. MOLDEN [42] was initially used for the structure generation and VMD [35] was used for structure visualization. The DFT simulations were run using norm-conserving Troullier-Martins pseudopotentials with double-zeta polarized basis sets. The K-grid cut-off was chosen to be 10 Å with a mesh cut-off of 800 Ry. An energy shift of 100 meV was used with a maximum force tolerance of 0.005 eV/Å. The empty sH hydrate structure was first generated and then structure relaxation in SIESTA was done to optimize the unit cell. The new relaxed coordinates were then used to generate the filled hydrate structure and for each, a structure relaxation was first done, and the relaxed coordinates are used for the rest of the simulations.

For each sH hydrate structure, two types of simulations were done. The first one involved changing the unit cell volume and obtaining the total system energy that corresponds to it by fixing the unit cell parameters to values that are certain percentage of the equilibrium unit cell parameters (maintaining the lattice c/a ratio). In the second type of simulations, a uniform pressure was applied to the whole cell to obtain the corresponding energy, volume, and unit cell parameters. To study the compressional behaviour of the structures, three equation of states (EOS) were used to fit the energy-volume and pressure-volume data to obtain the isothermal bulk modulus (B_o), its first pressure derivative (B'_o), and unit cell equilibrium volume (V_o). The equations of state are the Murnaghan [43], Birch-Murnaghan [44], and Vinet [45]. The isothermal EOS can be further developed to present the structure at high pressures and temperatures [31, 46].

Results and Discussion

Exchange-Correlation (XC) Functional

Generalized Gradient Approximation (GGA) exchange-correlation functionals have proved their adequacy for the DFT computations of different systems. Previous DFT studies of sI [38] and sII [31] gas hydrates that used GGA-revPBE [37] as XC functional were in good agreement with experimental findings. This was why this functional was selected here for DFT computations of sH hydrate systems. However, as mentioned above, since this functional doesn't account for the dispersion forces specifically those of guest-host interactions, vdW-DF DRSLL [39, 40] XC functional was also used to highlight the intensity of those interactions and their effect on sH hydrate structure and properties, relative to revPBE.

The total energy at equilibrium of sH hydrate systems using revPBE is around 0.7% higher than that obtained with DRSLL, that gives an indication that sH hydrate systems tend to have lower energy (and higher stability) when van der Waal forces are accounted for in DFT computations. The equilibrium volume was more affected by the XC functional type as it was found to be 1.2% higher when revPBE is used compared to DRSLL. This comparison excludes the empty sH hydrate system that showed higher dependency of its equilibrium volume on the XC functional type. Also, the equilibrium volume of the empty sH hydrate system with revPBE is around 5% lower than that with DRSLL, unlike the filled systems that showed the opposite trend. Among all systems, the equilibrium volume of the H_2-neohexane system was the least affected by the XC type and that of the Ar-neohexane was the most affected. These observations are also reflected on the computed density of sH hydrate systems that showed that systems are denser when DRSLL is used instead of revPBE (except for the empty system).

The unit cell parameters obtained with both functionals of four sH hydrate systems were compared to available experimental data at temperatures higher than 0 K. As Table I shows, the unit cell parameters obtained with DRSLL functional are closer to experimental ones than those of revPBE. revPBE tends to overestimate the values of lattice constants at 0 K as its results are equal to or greater than the experimental ones which are obtained at temperatures higher than 0 K. This agrees with Huo *et al.* [9] that found that revPBE XC functional tends to overestimate the values of unit cell parameters of sH hydrate compared to experimental values as it doesn't account for the guest-host van der Waal interactions. Comparing the results of unit cell parameters using revPBE and DRSLL revealed that for all the examined sH hydrate systems, the c-lattice constant is more affected by the XC type than the a-lattice constant. This was not the case for the Xe-neohexane sH structure that experienced the opposite. The c/a ratio was not

dependent on the XC type for the presented sH hydrate systems, except for the CH_4-neohexane sH structure that experienced a 1.5% higher c/a ratio when revPBE was used compared to DRSLL. Comparing the results of Ar-neohexane and CH_4-neohexane sH hydrate systems shows that the c-lattice constant of the CH_4-neohexane sH hydrate is greater than that of the Ar-neohexane hydrate which agrees with the experimental and MD results of Murayama *et al.* [15].

Table I: sH hydrate unit cell parameters obtained using two XC functionals as compared to experimental values.

	GGA-revPBE[a]		vdW-DRSLL[a]		Experimental		
sH hydrate	a, Å	c, Å	a, Å	c, Å	a, Å	c, Å	T, K
Ar + NH	12.33	9.78	12.27	9.72	12.16	9.93	93 [15]
CH_4 + NH	12.31	10.09	12.36	9.99	12.18	10.08	82 [47]
N_2 + NH	12.39	9.78	12.36	9.69	12.23	9.99	153 [48]
Xe + NH	12.47	10.09	12.40	10.09	12.29	9.99	110 [16]

a: DFT results at 0 K (this work)

NH: neohexane

The static pressure at equilibrium is also dependent on the XC functional type. For the empty, Ar-neohexane, and Xe-neohexane systems the equilibrium pressure obtained with revPBE was higher than that obtained with DRSLL. For the H_2-neohexane, CH_4-neohexane, and N_2-neohexane sH hydrate systems the equilibrium pressure obtained with revPBE was lower than that obtained with DRSLL. The dependence of sH hydrate equilibrium pressure on XC functional type depends on the type of guests that occupy the structure. The order of systems according to the dependency of their equilibrium pressure on XC functional type is as follows (in

ascending order), Ar-neohexane, empty, N_2-neohexane, H_2-neohexane, Xe-neohexane, CH_4-neohexane.

The type of guest molecules affects the equilibrium pressure of sH hydrate system at a given temperature. This was previously discussed by Ohmura *et al.* [49] and Murayama *et al*. [50] for sH hydrate systems. Analogous to this, it was interesting to observe the static pressure of neohexane sH hydrate systems at equilibrium 0 K conditions. It was found that the value of static pressure at equilibrium is dependent on the type of help gas molecules that occupy the small and medium cages; conversely, this dependency was different between the two used functionals. The help gas molecules increase the static pressure at equilibrium of neohexane sH system in the following ascending order when revPBE is used; Nitrogen, Argon, Hydrogen, Methane, and Xenon. However, the order is different for the DRSLL results and it is: Xenon, Argon, Nitrogen, Hydrogen, and Methane.

Figure 2 represents the compressional behaviour and volume response to pressure of sH hydrate systems with and without van der Waal forces (i.e. DRSLL and revPBE, respectively). As shown, this behaviour is consistent for all filled systems at 0 K. However, the empty sH system shows a deviation from other systems for tensile pressures less than -0.7 GPa. This kind of deviation was not observed when revPBE was used as XC functional.

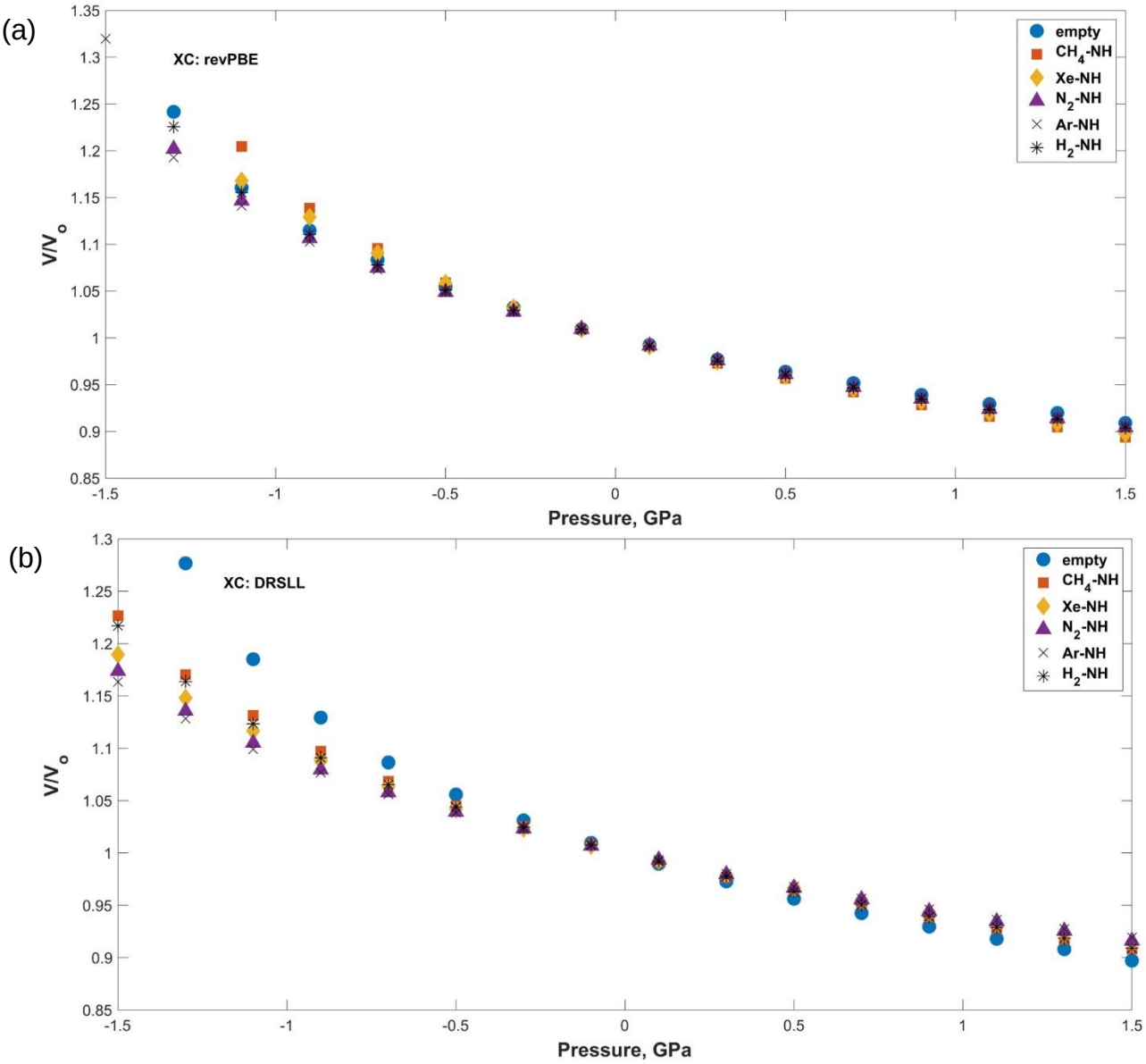

Figure 2:(a) Volume-pressure data for sH hydrate systems using revPBE functional. (b) Volume-pressure data for sH hydrate systems using DRSLL functional.

The differences in compressional behaviour of each sH hydrate system between revPBE and DRSLL XC functionals was examined and a noticeable difference in volume response to pressure between the two functionals was found for all sH hydrate systems at tensile pressures ≤ -0.7 GPa. For systems such as Ar-neohexane, H_2-neohexane, and empty sH structures, the

deviation was obvious at pressures ≤ -1.1 GPa. This reflects that the maximum tensile pressure @ 0 K obtained from DFT for sH hydrate depends on the XC type. The hydrate systems with revPBE tend to deform under tensile pressures less than or equal to those when DRSLL is used. This suggests that sH hydrate systems exhibit higher mechanical strength when van der Waals interactions are accounted for in DFT simulations as shown in the CH_4-neohexane sH example in Figure 3. The effect of XC functional type has been observed for different sH hydrate structure properties as will be highlighted in next sections.

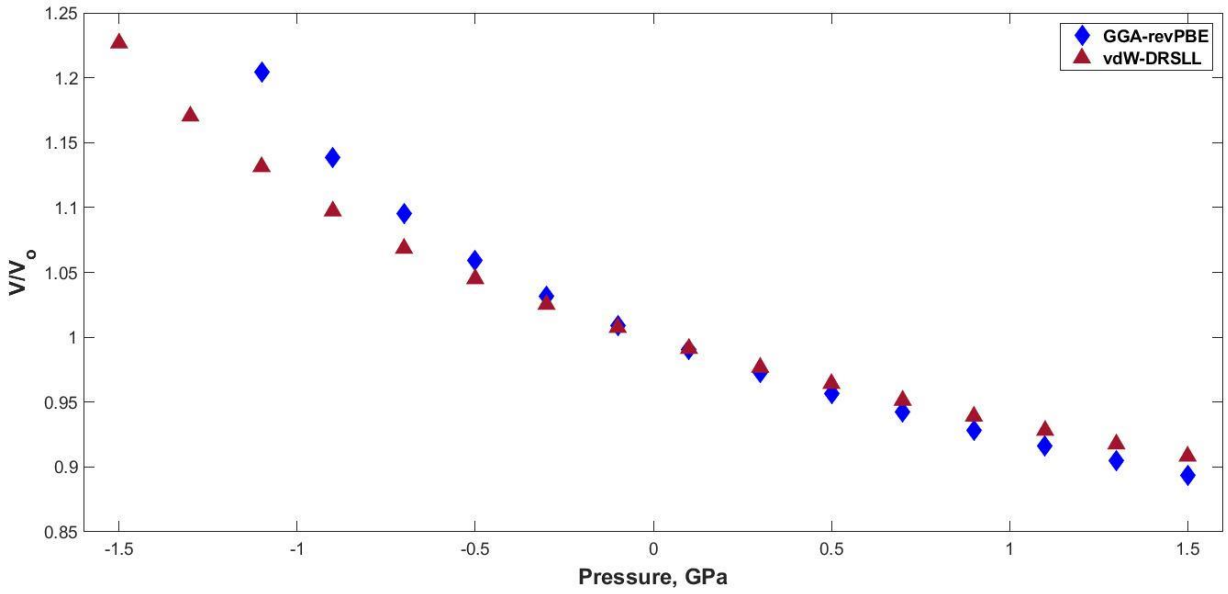

Figure 3: Volume-pressure curve of CH_4-neohexane sH hydrate using two XC functionls.

Equation of State (EOS) Fitting

The isothermal equation of state fitting was done for the six systems involved in this study using three different EOS: Murnaghan, Birch-Murnaghan, and Vinet. For each EOS, both energy explicit and pressure explicit forms were used to fit energy-volume and pressure-volume data, respectively.

The energy-volume data were obtained by changing the unit cell volume, allowing the structure to relax, and obtaining the corresponding minimum total energy of the system. The length of the unit cell parameters (a, b, c) were changed while maintaining the optimum c/a ratio for each system. A representative example of Vinet equation of state fitting of the energy-volume data of the CH_4-neohexane sH hydrate system is presented in Figure 4.

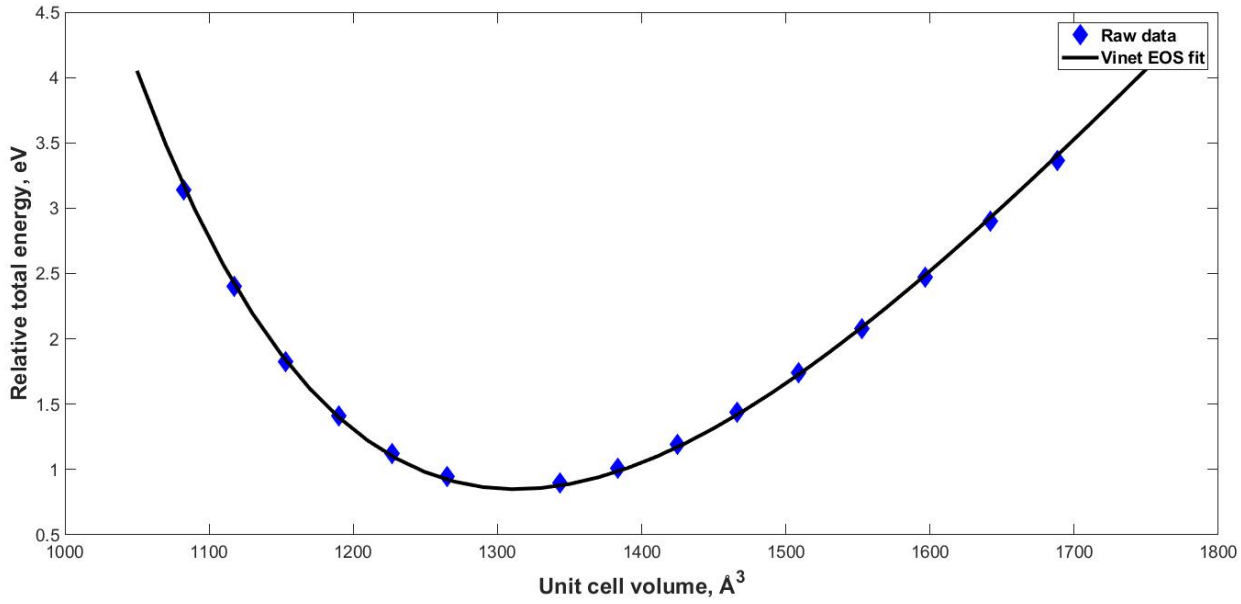

Figure 4: Energy-volume curve of CH_4-neohexane sH hydrate obtained with vdW-DRSLL XC functional and fitted using Vinet EOS.

The fitting parameters of the three equation of states are the equilibrium volume V_o, the isothermal bulk modulus B_o, and the first pressure derivative of the bulk modulus B'_o. Table II presents an example of the computed parameters for the CH_4–neohexane sH hydrate system using the three equations of states, two XC functionals, and at two pressure ranges at 0 K.

Table II: EOS parameters of the CH_4-neohexane sH hydrate obtained using two XC functionals at 0 K: equilibrium unit cell volume V_o ($Å^3$), isothermal bulk modulus B_o (GPa), and the pressure derivative of bulk modulus B'_o.

	Exchange-Correlation Functional					
	GGA-revPBE			**vdW-DRSLL**		
Equation of State	(-1.24 to 3.99 GPa)			(-1.65 to 3.82 GPa)		
	V_o	B_o	B'_o	V_o	B_o	B'_o
Murnaghan	1325.78	9.57	5.59	1313.92	11.97	4.92
Birch-Murnaghan	1325.24	9.96	5.59	1315.11	12.23	4.72
Vinet	1325.39	10.02	5.55	1312.65	12.67	4.93
	(-1.10 to 1.50 GPa)			(-1.50 to 1.50 GPa)		
	V_o	B_o	B'_o	V_o	B_o	B'_o
Murnaghan	1324.50	9.73	5.66	1307.22	12.16	5.35
Birch-Murnaghan	1324.48	9.92	5.52	1307.60	12.30	5.10
Vinet	1324.53	9.96	5.47	1307.76	12.35	5.01

The results of the computed parameters of the six sH hydrate systems presented in this study showed that the differences between the results of the three EOS using the same exchange-correlation functional are smaller than those of the same EOS using different functional which agrees with the findings of Vlasic et al. [31] for sII hydrate structure at 0 K. The changes between the semi-local GGA-revPBE functional that doesn't account for the guest-host dispersion interactions and that of the non-local vdW-DRSLL functional revealed the sensitivity of EOS parameters to the type of XC functional used. The results of all systems revealed that the isothermal bulk modulus and its pressure derivative (Bo and B'o) are affected by the type of the

XC functional more than the equilibrium volume Vo. Bo is higher when DRSLL is used instead of revPBE for the "filled" sH hydrate systems, which shows that the van der Waal forces - which are accounted for in this functional – increased the compressional resistivity of those sH hydrate structures. The opposite was observed for the empty sH structure that has lower Bo when DRSLL is used.

The XC functional type has its effect on the first pressure derivative of the isothermal bulk modulus (B'_o). Figure 5 shows that B'_o obtained with DRSLL is lower than that obtained with revPBE. DRSLL results demonstrate that the empty sH hydrate system has the lowest B'_o, and it increases with increased sH hydrate density, not with increased guest size as was previously found by Vlasic *et al.* [31] using revPBE. The revPBE results of this work show an opposite trend to that of DRSLL with B'_o being less dependent on hydrate density and is maximum for the empty sH hydrate. This requires an addition attention to this EOS parameter that has been previously taken as a constant value of 4.0 for gas hydrate studies [51, 52, 53].

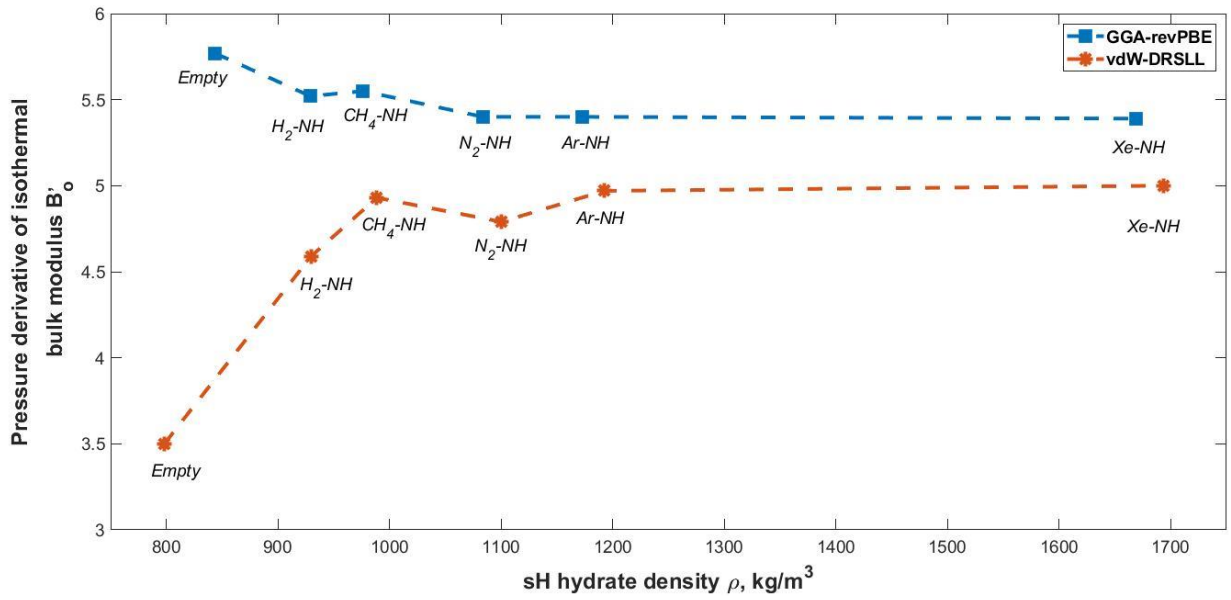

Figure 5: Effect of sH hydrate density on its pressure derivative of isothermal bulk modulus B'_o at 0 K. Results obtained with Vinet EOS.

Observing the effect of changing the pressure range on EOS fitting results shows that the equilibrium volume V_o is the least affected parameter by pressure range changes. This agrees with a previous work of Vlasic *et al.* [31] that involved sII hydrate systems at 0 K. The isothermal bulk modulus sensitivity to pressure range changes differs based on the XC functional type and the guests that the system encapsulates. The empty, CH_4-neohexane, N_2-neohexane, and H_2-neohexane sH systems exhibit larger changes in B_o with pressure range when DRSLL is used as XC functional. On the other hand, B_o of the Xe-neohexane and Ar-neohexane is more sensitive to pressure range changes when revPBE is used as XC functional. The pressure derivative of the isothermal bulk modulus of the empty, CH_4-neohexane, and H_2-neohaxane sH hydrate systems is more affected by the pressure range change when DRSLL is used, however, revPBE causes different sensitivity of B'_o to pressure range for the Xe-neohexane and the Ar-neohexane systems as their sensitivity differs by EOS. The N_2-neohexane experienced an equal change of B'_o with pressure using both XC functionals.

The three EOS used in this study are considered adequate for the isothermal fitting of energy-volume and pressure-volume data of sH hydrate systems. However, some of the EOS perform better with changing pressure conditions than others depending of the type of help gas and the type of XC functional used. This agrees with the work of Vlasic *et al.* [31] that discussed how hydrate systems should be treated on case by case basis when it comes to isothermal EOS fitting. An example is the CH_4-neohexane sH hydrate system parameters obtained by Birch-Murnaghan EOS which are the least affected by changes in pressure range when revPBE is the XC functional. On the other hand, parameters obtained from Vinet EOS for the same system when DRSLL is the XC functional are the least affected by pressure range variation. For the N_2-neohexane sH system, parameters from Murnaghan EOS were less affected by pressure range

change than other equations of state when revPBE is the XC functional, but Vinet EOS performed better when DRSLL was used.

The empty sH hydrate system is unique in its compressional behaviour and response to variations in pressure range when compared to filled sH systems. When revPBE was used as the XC functional of this system, the EOS parameters response to pressure range changes agreed with those of other systems, however, when DRSLL was used both of B_o and B'_o showed substantial dependence on pressure range.

Structure – H Hydrate Geometry and Density

As above-mentioned the computation of some of the mechanical properties of sH hydrate systems was done using DFT and two exchange-correlation functionals. The results are presented in Table III using revPBE and DRSLL with Vinet EOS. Since the same LGMS was used in all sH hydrate systems presented here (NH: neohexane), it was interesting to observe the effect of the help gas on sH hydrate properties. As shown in Figure 6, as the size of the help gas increases, the equilibrium volume of the whole sH structure increases which agrees with the DFT results of sII gas hydrates of Vlasic *et al.* [31] and the molecular dynamic simulations of gas hydrates of Zele *et al.* [54]. The structure-H density was directly affected by the molar mass of help gas as it was minimum for the H_2-neohexane system and maximum for the Xe-neohexane system. Figure 7 presents a linear relationship of neohexane sH hydrate structure that can be used to estimate the density of this structure with different help gas molecules using their molar mass.

Table III: sH hydrate properties at 0 K computed with two XC functionals and Vinet EOS.

	GGA - revPBE					
	Empty	**H_2 - NH**	**CH_4 - NH**	**N_2 - NH**	**Ar - NH**	**Xe - NH**
V_o (Å^3)	1205.92	1266.66	1324.97	1285.22	1272.12	1348.18
ρ (kg/m^3)	843.44	929.08	976.18	1083.72	1172.79	1669.17
a (Å)	11.93	12.34	12.31	12.39	12.33	12.47
c (Å)	9.76	9.74	10.09	9.78	9.78	10.09
c/a	0.82	0.79	0.82	0.79	0.79	0.81
B_o (GPa)	11.49	11.37	10.02	11.65	11.95	10.17
B'_o	5.77	5.52	5.55	5.40	5.40	5.39
h (bond/ Å^3)	0.0564	0.0537	0.0513	0.0529	0.0535	0.0504
	vdW - DRSLL					
	Empty	**H_2 - NH**	**CH_4 - NH**	**N_2 - NH**	**Ar - NH**	**Xe - NH**
V_o (Å^3)	1274.36	1265.88	1308.27	1265.86	1250.88	1328.99
ρ (kg/m^3)	798.14	929.66	988.64	1100.29	1192.71	1693.27
a (Å)	12.10	12.34	12.36	12.36	12.27	12.40
c (Å)	9.96	9.70	9.99	9.69	9.72	10.09
c/a	0.82	0.79	0.81	0.78	0.79	0.81
B_o (GPa)	9.39	12.28	12.67	13.91	14.60	13.41
B'_o	3.50	4.59	4.93	4.79	4.97	5.00
h (bond/ Å^3)	0.0534	0.0537	0.0520	0.0537	0.0544	0.0512

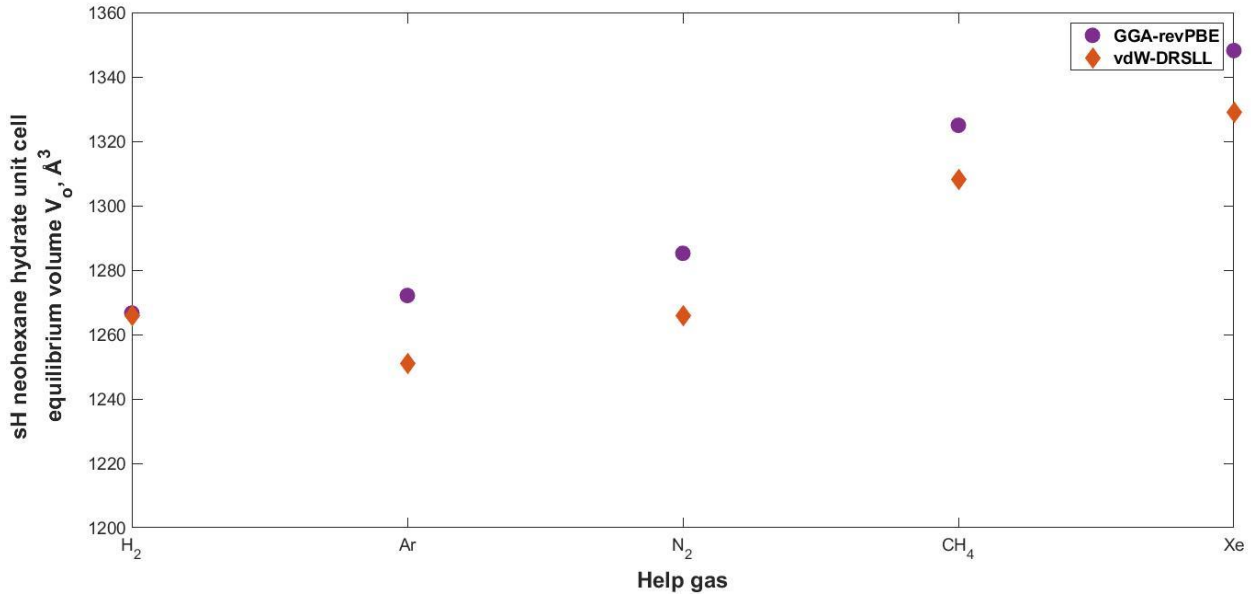

Figure 6: Effect of help gas size on sH hydrate equilibrium volume V_o.

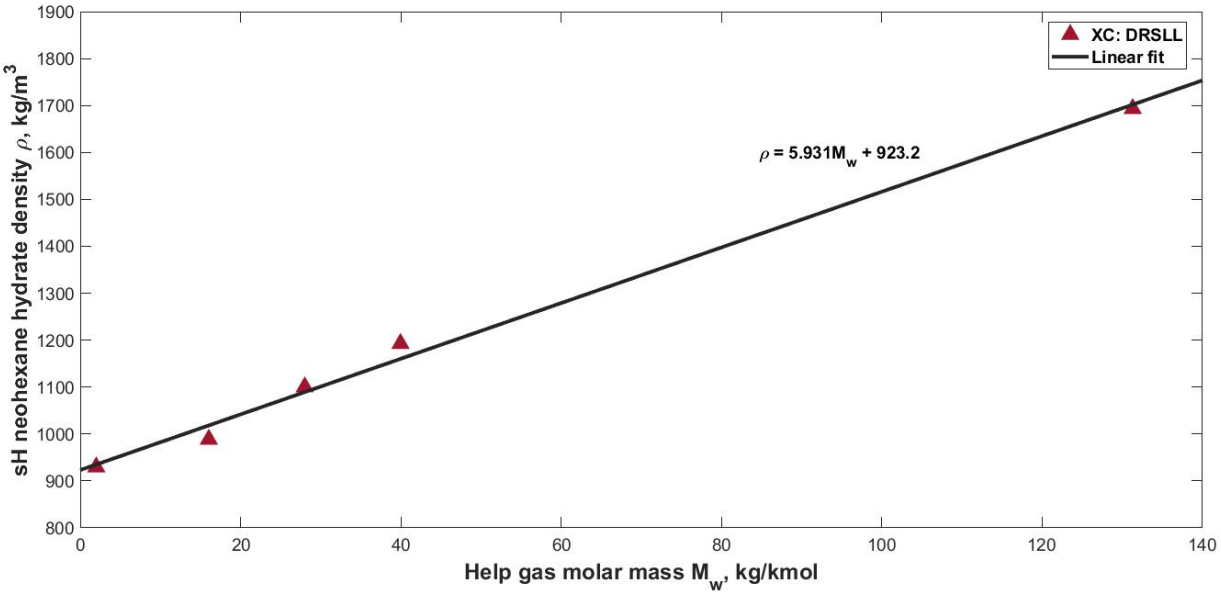

Figure 7: sH hydrate density vs. help gas molar mass obtained with DRSLL XC functional.

The size of the help gas encapsulated in the medium and small cages of the neohexane sH structure was found to increase the a-lattice and c-lattice unit cell parameters as well as the c/a ratio of the sH hydrate structure. Observing the results of these parameters that were obtained using revPBE and DRSLL XC functionals shows that the a-lattice constant computed with

DRSLL is less than that computed with revPBE except for the H_2-neohexane sH hydrate, were both values are equal, and the CH_4-neohexane + the empty sH system with a-lattice $_{DRSLL}$ > a-lattice $_{revPBE}$. Similarly, the c-lattice constant calculated with DRSLL is less than that calculated with revPBE except for the Xe-neohexane sH hydrate (both are equal), and the empty sH system with c-lattice $_{DRSLL}$ > c-lattice $_{revPBE}$. This leads to having c/a $_{DRSLL}$ ≈ c/a $_{revPBE}$ except for the CH_4-neohexane and N_2-neohexane sH structures (c/a $_{DRSLL}$ < c/a $_{revPBE}$).

Isothermal Bulk Modulus

The isothermal zero-pressure bulk modulus (B_o) is a property of the material that depends on different factors. Bulk modulus depends on the crystal structure and the chemical composition of the material [55]. For gas hydrates, the bulk modulus is one of the properties that can be influenced by different factors such as the hydrogen bonds of the host lattice and the type, size, and shape of the guest molecules. For the six sH hydrate systems presented in this work, the effect of help gas size and chemistry, hydrate density, and hydrogen-bond density on B_o was observed. The discussion of these observations follows in next sections.

Effect of Help Gas on sH Hydrate Isothermal Bulk Modulus (B_o)

Figure 8 presents the isothermal bulk modulus of the filled neohexane sH hydrate systems with different help gas sizes. As was previously highlighted, B_o is higher when DRSLL is used as the XC functional (excluding the empty system). Figure 8 highlights the effect of the XC functional type on the calculated isothermal bulk modulus. It shows that this effect is pronounced for some systems compared to others. For example, B_o of the H_2-Neohexane hydrate is the least affected by the XC functional type while that of the Xe-neohexane sH hydrate is the most affected by the XC functional type. This could be an indication of the intensity of the dispersion interactions that

guest molecules have with host water cages. Figure 8 also reflects how van der Waal interactions (DRSLL) define the hydrate incompressibility, while revPBE simply shows that the larger the size of the help gas (and hence V_o), the lower is the hydrate bulk modulus B_o (higher compressibility). The isothermal bulk modulus (B_o) results obtained with and without van der Waal interactions changed the order of resistance to uniform compression that the investigated systems have.

When accounting for van der Waal interactions (DRSLL), the increasing order of the systems in terms of B_o is: empty < H_2-NH < CH_4-NH < Xe-NH < N_2-NH < Ar-NH, while the increase in order of B_o when revPBE is used (no dispersion interactions) is: CH_4-NH < Xe-NH < H_2-NH < empty < N_2-NH < Ar-NH. The common conclusion between the results of both XC functionals is that the following systems are ordered in ascending order in terms of B_o: CH_4-NH < Xe-NH < N_2-NH < Ar-NH. To explain this order a knowledge of the chemistry of the help gas molecules is required. The CH_4-NH sH hydrate has the lowest B_o among the four systems which might be due to the tetrahedral geometry and orientation of methane molecule which weakens the hydrogen bonds of the host structure and hence increases its compressibility (and decrease its B_o). Moreover, for previous studies of sI hydrate, it was found that the binding energy of methane molecules in the 5^{12} cages is lower than that of xenon in the same cage [56]. It was also found that methane has higher binding energy than hydrogen molecules in the 5^{12} cages [57]. The higher binding energy is consistent with higher bulk modulus (B_o) of this work which agrees with the conclusion found by Jendi *et al.* [38] for CH_4 and CO_2 sI hydrates. The quadrupole moment that nitrogen molecule has contributes to the intermolecular interactions that it has with host water cages which can explain its high bulk modulus compared to other systems. The neohexane sH hydrate is highly resistive to compression when argon is encapsulated in its

medium and small cages. Although argon is a noble, non-polar spherical element [58], it has been identified to have dispersive interactions with water molecules. These interactions are affected by the variations of the electron structure of water molecule compared to methane - water interactions which can be linked to the electron delocalization of the hydrate hydrogen bonds that affects the guest-host interactions [59]. This can explain the high bulk modulus of Ar-NH sH hydrate structure compared to others presented in this work. The results presented in this work for the CH4-neohexane system are comparable to the work of J. Liu, et al. [60] who simulated different sH hydrate systems using DFT with GGA-PBE exchange correlation functional and AIMD and 260 K. The bulk modulus calculated by J. Liu, et al. [60] for the sH hydrate containing methane as help gas and three ethane molecules in the large cage is 9.859 GPa, while that containing two propane molecules in the large cage and methane as help gas is 9.452 GPa. These values are close to that of the CH4-neohexane system simulated in this work using GGA-revPBE with bulk modulus of 9.96 – 10.02 GPa. It was noticed that the number of carbons in the large cage is the same for those three systems which can explain the closeness in results of the calculated bulk modulus. The unit cell volume results of Xe-neohexane sH hydrate computed in this work using both XC functionals compare well with the experimental work of Alavi, Ripmeester, and Klug [14] at 40 K and 1 atm. Their work involved multiple occupancy of the rare gas in large cage of sH hydrate. The unit cell volume of Xenon sH hydrate with 4 Xenon atoms in the large cage was found to be 1312.6 Å3, while that of sH hydrate with 5 Xenon atoms in the large cage was found to be 1348.6 Å3. This compares to the unit cell volume of Xe-neohexane found this work and presented in Table III.

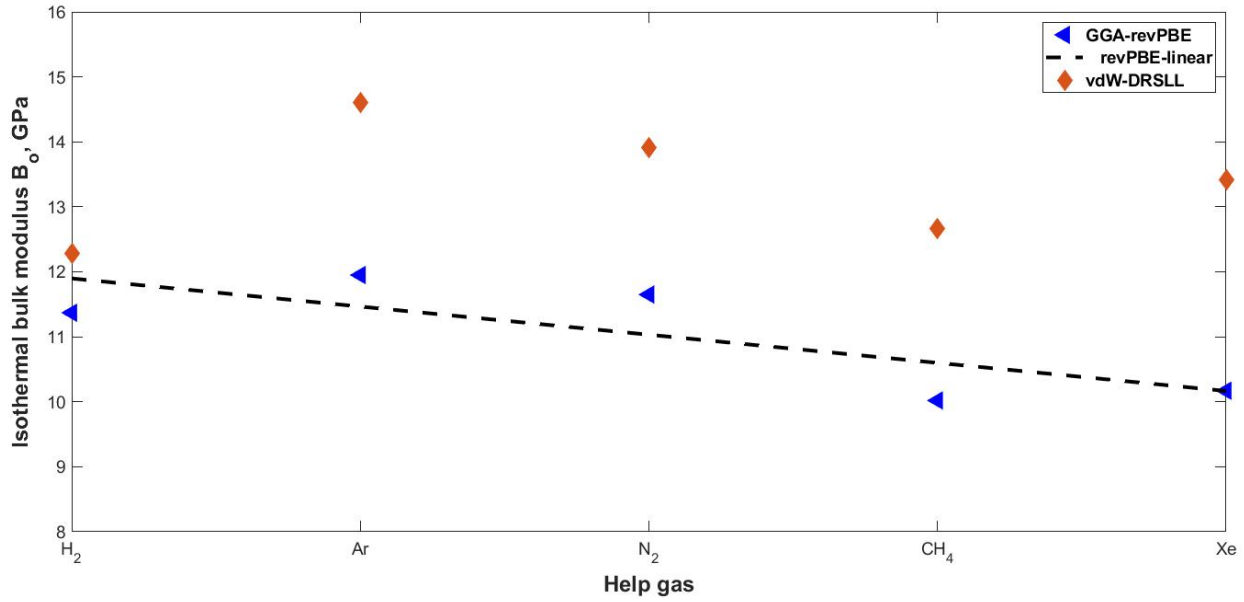

Figure 8: Effect of help gas size on neohexane sH hydrate isothermal bulk modulus.

Effect of Hydrate Density on B_o

The effect of sH system density and specific volume on B_o is presented in Figure 9 and Figure 10, respectively. The results using both functionals show that there is an exponential relationship between the hydrate density and its isothermal bulk modulus. The denser is the system the higher its B_o and hence its degree of incompressibility. The data are better correlated when van der Waal forces are accounted for using DRSLL XC functional. The Xe-neohexane sH hydrate doesn't fit into this correlation, despite its high density its isothermal bulk modulus B_o is lower than some of the systems with much lower density. Similarly, the isothermal bulk modulus versus sH hydrate specific volume was correlated (Figure 10) and an exponential relationship is obtained. The results found here essentially agree with a previous work of Anderson [61] that showed how the bulk modulus of oxide compounds decreases with increased specific volume of ionic crystals.

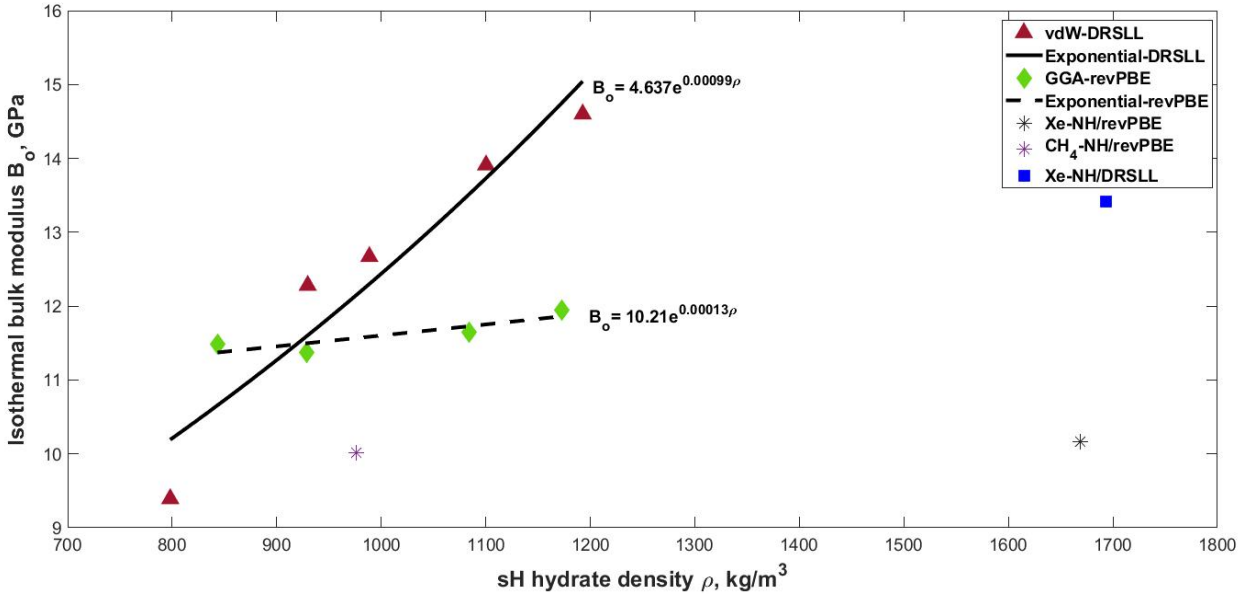

Figure 9: Isothermal bulk modulus vs. density of sH hydrate

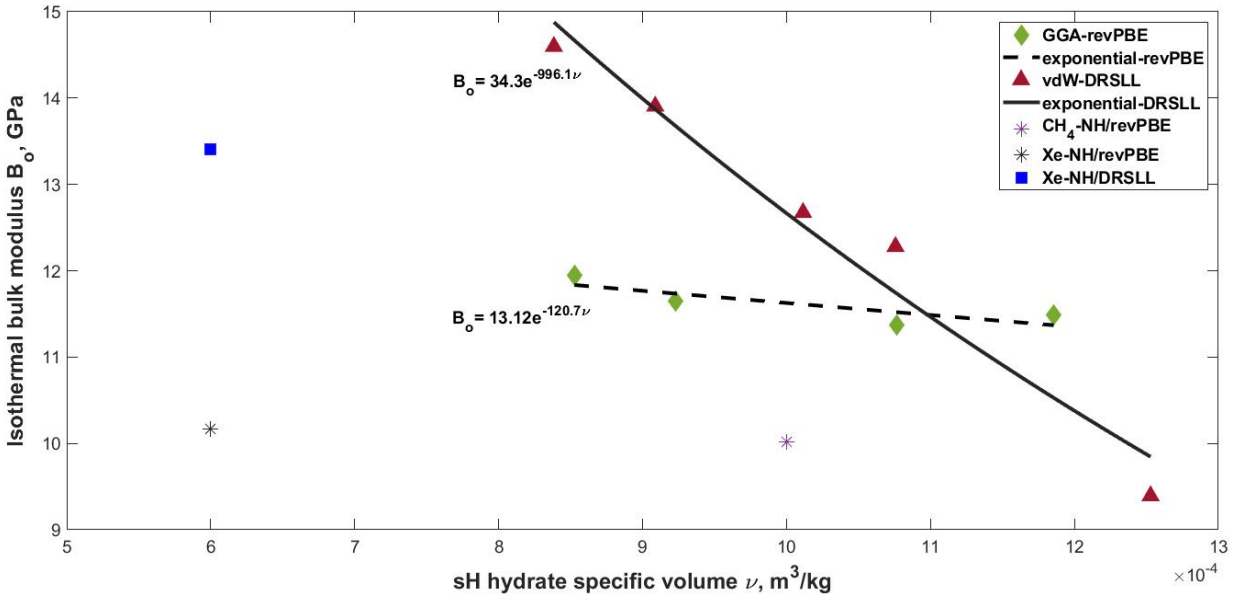

Figure 10: Isothermal bulk modulus vs. specific volume of sH hydrate.

Effect of Hydrogen-Bond Density on B_o

As is well-known, the hydrogen bond is a unique characteristic that enables water molecules to

create the backbone of hydrates structure. The energy of this bond was previously believed to be electrostatic, however, it was found that quantum charge-transfer, dispersion, and delocalization are important contributors to the hydrogen bond energy [62, 63]. The work of Manakov *et al.* [53] concluded that the elasticity of the gas hydrate structure determines the hydrate resistance to uniform compression (bulk modulus). The work of Vlasic *et al.* [31] on sII hydrate structure showed how the isothermal bulk modulus (B_o) of sII hydrate encapsulating hydrocarbon molecules depend directly on the density of hydrogen bonds in a structure.

Table III and Figure 11 demonstrate the effect of hydrogen bond density (h = # H-bonds/unit-cell volume, $Å^3$) on isothermal bulk modulus at 0 K of sH hydrate. When van der Waal interactions were not accounted for in DFT computations (XC: revPBE), the results show that there is an increase of sH hydrate bulk modulus (B_o) with increased hydrogen bond density. However, when van der Waal interactions are in effect (XC: DRSLL) the relationship between bulk modulus and hydrogen bond density is not direct. It is critical to notice that the guest molecules that Vlasic *et al.* [31] managed to fit into a correlation that relates B_o to H-bond density belong to the same family of chemical components (hydrocarbons). On the other hand, the guest molecules studied in this work don't belong to the same family.

Each sH hydrate system in this work is individual in its characteristics and this individuality is more pronounced when van der Waal forces where used. What is agreed on is that hydrogen bond density affects the bulk modulus of sH hydrate, however, when van der Waal forces are present, they also have their effect on bulk modulus [53]. When DRSLL is used, both H_2-neohexane and N_2-neohexane sH hydrates have almost the same H-bond density and yet the N_2-neohexane sH hydrate has an isothermal bulk modulus that is 13% higher than that of the H_2-neohexane hydrate. This is an indication of the importance of accounting for the van der Waal

forces in hydrate DFT simulations to avoid underestimating its properties. What seems obvious from Figure 11 is that bulk modulus obtained with revPBE XC functional are better correlated with the H-bond density of the hydrate system than those of DRSLL. However, as Figure 9 shows, B_o obtained with DRSLL is better correlated with the hydrate density than that obtained with revPBE.

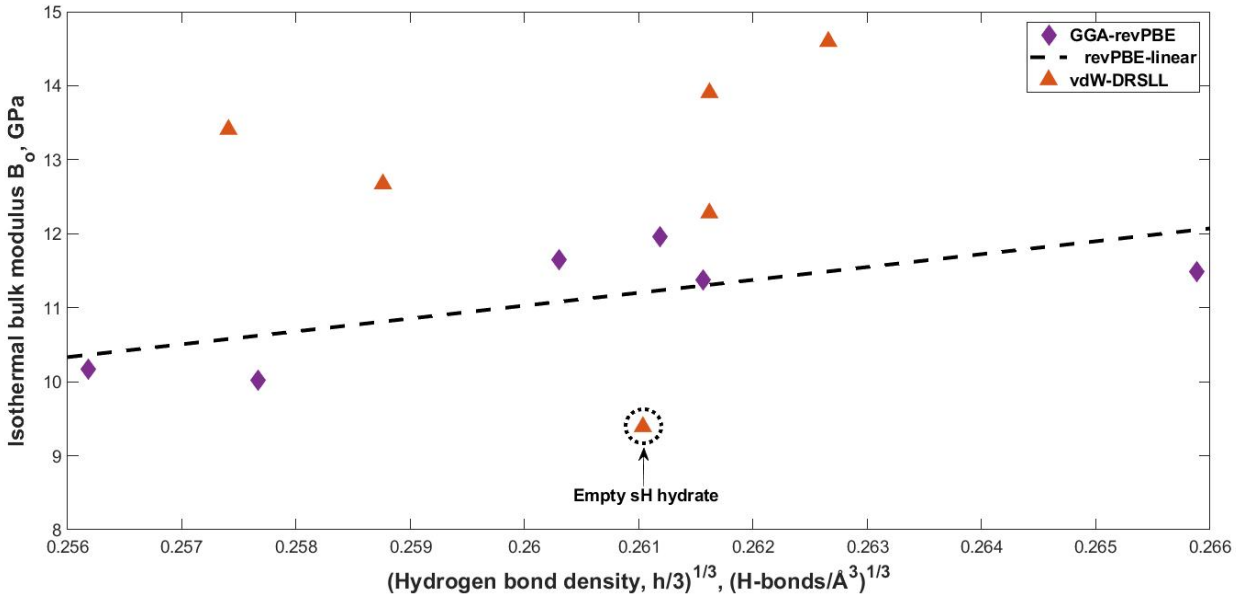

Figure 11: Effect of hydrogen bond density on sH hydrate isothermal bulk modulus using two XC functionals and Vinet EOS.

Structure-H Hydrate Anisotropy

Structure-H hydrate has been identified by its anisotropy which makes it unique compared to the relatively isotropic cubic structures of sI and sII. Gudkovskikh and Kirov [64] have found that the universal anisotropy index of sH hydrate is much higher than that of structures sI and sII. The six systems presented here are used to investigate the level of structural anisotropy that structure H hydrate has by observing the compressional response of the a-lattice and the c-lattice constants. Figure 12 shows the change in the a-lattice and c-lattice constants of sH hydrate with pressure at 0 K, respectively. Figure 12 presents the results obtained with van der Waal forces

using DRSLL functional.

As Figure 12 highlights, the a-lattice constant increases with the filling of the sH structure and is maximum for the structures encapsulating the large help gas molecules (Xe, CH_4). The same behaviour was observed for the change of the c-lattice constant with pressure except for the empty sH structure that has a c-lattice constant that is higher than three of the filled systems. The effect of the help gas molecule size on the lattice constants was clearly observed for pressure > 0 GPa. The c/a ratio was also found to be decreasing with increased uniform pressure for all investigated systems except for the empty sH hydrate (using both functionals) and the CH_4-neohexane sH hydrate (using revPBE only). Murayama *et al.* [15] had previously investigated the anisotropic lattice expansion of structure H hydrate using experiments and MD simulations. They found that the a-lattice constant was not affected by the size of the help gas molecule unlike the c-lattice constant. The temperature range they worked with was 93-183 K and they had three systems in that study. Tse [16] had a similar analysis for two different sH hydrates and showed that their thermal expansion is anisotropic. For a temperature range of 75 – 225 K, Tse showed experimentally that the change of the c-lattice constant with temperature is less than that of the a-lattice constant.

In this work the effect of pressure on the unit cell parameters of six sH hydrate systems was studied. It was found that the change of the a-lattice constant with pressure is higher than that of the c-lattice constant. This shows that sH hydrate systems are less compressible along the c-direction. This anisotropy was not observed for the N_2-NH and H_2-NH sH hydrate systems in which both axes respond equally to changes in pressure. The effect of the XC functional was noticed in this analysis as the results of revPBE reflected higher changes in the unit cell parameters with pressure more than that obtained with DRSLL (except for the empty system).

This proves the role of van der Waal forces in increasing the stability of sH hydrate structure under applied tensile and compression pressure. The effect of XC functional type on the directional compressional behaviour of sH hydrate was pronounced for the Ar-NH hydrate and was the least noticeable for the H_2-NH hydrate. Small variations in unit cell parameters response to pressure were observed for the different help gas sH hydrate systems. This suggests that the type, shape, size, and interactions of guest molecules contribute to the level of anisotropy that sH hydrate has. This agrees with findings of Takeya *et al.* [17] who investigated experimentally the unit cell parameters of sH hydrate using different LGMS and found that the a-lattice constant increases while the c-lattice constant decreases with increased size of the LGMS. Vlasic *et al.* [65] also demonstrated how the level of anisotropy of sII gas hydrate is dependent on the size of guest molecules using first principle computations.

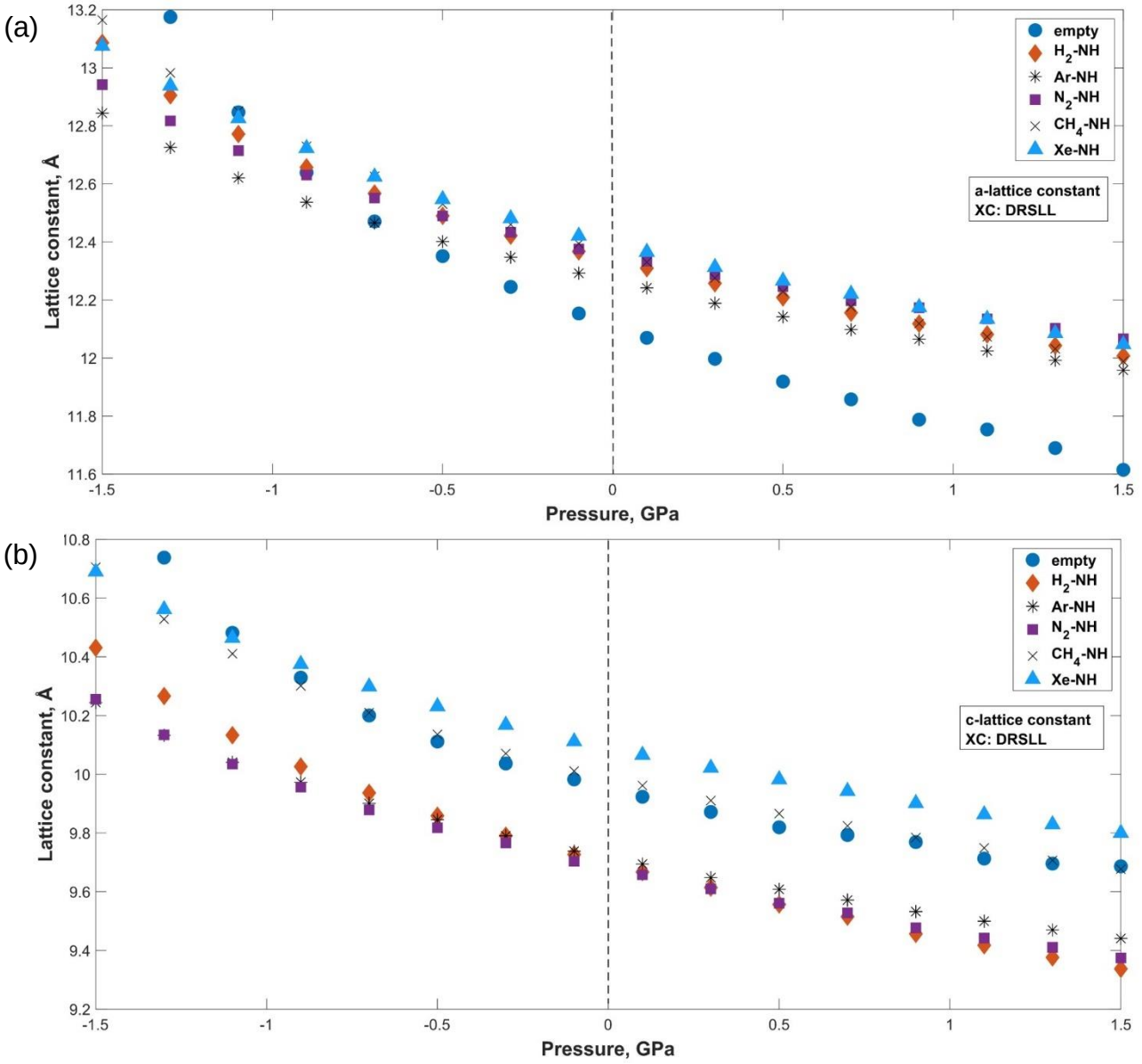

Figure 12: (a) Change of sH hydrate a-lattice constant with applied pressure. (b) Change of sH hydrate c-lattice constant with applied pressure.

Comparative Analysis

This work is a reflection on some of the properties of sH hydrate obtained from first principle computations. In this section we highlight some of the similarities and unique characteristics that sH hydrate has compared to sI, sII, and ice (Ih). This structure is the smallest in size compared to

sI and sII hydrate with 34 water molecules per unit cell. Its size is closer to sI (46 water molecule) than it is to sII (136 water molecule). The density found for filled sH hydrate systems studied in this work are in the range of 929 – 1,693 kg/m^3 depending on the type of guest molecules. The density of sI methane hydrate was found to be 943 kg/m^3 [38] and that of sII filled with hydrocarbons is in the range of 932.4 – 960.9 kg/m^3 [31]. Those values are comparable to the H_2-neohexane and CH_4-neohexane sH hydrate densities. The density of empty sH hydrate is comparable to that of empty sII found by Vlasic *et al.* [31]. The structure of sH hydrate differs from those of sI and sII by being a hexagonal structure with higher anisotropy. The length of the a-lattice constant of sI methane hydrate was found to be 11.90 Å using DFT computations [38], while that of methane-neohexane sH hydrate was found in this work to be around 12.33 Å. Unlike sI and sII hydrates, sH is known for having a c-lattice constant that is less than its a-lattice constant. The optimum c/a ratio of the sH hydrate systems presented here was found to range between 0.78 and 0.82 depending on the type of guest molecules. The isothermal bulk modulus of methane sI hydrate was found from DFT computation (XC: revPBE) to equal 9.98 GPa [38] which close the isothermal bulk modulus found for methane-neohexane sH hydrate (10.02 GPa) using the revPBE. Our results of B_o (using revPBE) are compared to those of Vlasic *et al.* [31] who used the same XC functional to estimate B_o for different sII hydrate systems. The isothermal bulk modulus of empty sH hydrate is almost the same as that of sII, however, B_o of filled sH systems is higher than that of sII systems filled with hydrocarbons. This reflects that sH hydrate system could be more resistive to uniform compression than sI and sII hydrates which might be due to different factors such as the structural anisotropy imposed by the hexagonal lattice structure.

Since sH hydrate has a hexagonal structure, it would be interesting to compare its properties to those of hexagonal (Ih) ice. In terms of density, the structure of empty sH hydrate is less dense than that of ice Ih with reported value of density of 937 kg/m^3 (experimental @ 237.5 K) [66], and 933 kg/m^3 (hybrid DFT @ 273 K) [27]. What is common between sH and (Ih) ice structures is that the a-lattice and c-lattice constants are unequal unlike the cubic structures of sI and sII hydrates. The average c/a ratio of sH hydrate systems studied in this work is 0.80 while that of ice Ih is 1.622 [67]. The average a-lattice and c-lattice parameters of sH hydrate were found in this work to be 12.30 Å and 9.86 Å, respectively while those of ice Ih are 4.52 Å and 7.36 Å (@ 273 K) [5]. The bulk modulus of sH hydrate was found to be dependent on the type of guest molecules. DFT computations revealed that this measurement of hydrate incompressibility is sensitive to the density of hydrogen bonds as well as the guest-host interactions. An average of isothermal bulk modulus of 12.71 GPa (DRSLL & Vinet EOS) was estimated for the sH hydrate structures investigated in this work at 0 K. A bulk modulus of 7.81 GPa of ice (Ih) was reported by Jendi *et al.* [67] using first-principle computations. Depending on the temperature, other values were reported in literature for the bulk modulus of ice (Ih) such as 9.61 GPa (@ 237.5 K) [66] and 8.8 GPa (@ 272 K) [5]. This indicates that sH hydrate can be more incompressible than ice (Ih) depending on the type of guest molecules that are captured inside its cages.

Conclusions

In this work we have characterized, analysed and partially validated several important mechanical properties of sH hydrate at the atomistic level using DFT at 0 K. Scarcity of theoretical, experimental and simulation data prompts the need to simulate and explore their material parameter space with methods that account for different degrees of interactions. Two types of exchange-correlation functionals were used to perform the molecular simulations.

Results reflects the role of van der Waal forces that molecules in a structure experience which affects materials properties and response to compression. The properties of six sH hydrate structures were determined reflecting on how they are affected by the XC functional and the help gas type. Isothermal equation of state fitting was done using three different EOS which revealed that results were more sensitive to the XC type than the type of EOS used. The sensitivity of EOS fitting parameters to pressure range changes is a key factor that can determine the most suitable EOS to fit the data of an sH hydrate structure.

The role of van der Waal forces was pronounced in the higher bulk modulus obtained for the filled sH hydrate structures studied here. This highlights the importance of the XC functional selection that suits the hydrate structure to make sure that its properties are accurately estimated. DFT simulations with the van der Waal non-local XC functional (DRSLL) gave geometrical results that are closer to available experimental data than those of revPBE. However, both functionals perform well in determining sH hydrate properties at the atomistic level. The difference in results between the two functionals was also a function of the type of help gas molecules. This requires a closer attention to the geometry and chemistry of these molecules as they define the interactions that molecules have with the host water structure, and hence govern the hydrate properties and its stability limits. With van der Waal forces in place, sH hydrate structures were found to be denser and more resistive to uniform compression as well as having an isothermal bulk modulus that is highly dependent on the hydrate density and the type of guest molecules it encapsulates, and less dependent on hydrogen bond density alone.

The structural anisotropy of sH hydrate was noticeable in the difference in response to pressure and compressibility between its unit cell parameters. This directional dependency was also a function of the type of help gas that occupies the small and medium cages of this hydrate

which reflects the importance of understanding the chemistry and composition of hydrate structures to accurately determine the properties needed for their development for different applications. The points of uniqueness and similarities of sH hydrate as compared to sI and sII hydrates as well as ice (Ih) were briefly highlighted and quantified.

Taken together the present work contributes to the evolving understanding and characterization of the structure-chemistry-property relations of these anisotropic gas hydrates and to the development of a computational material science platform for this complex crystal.

Acknowledgements

This work was supported by the Natural Sciences and Engineering Research Council (NSERC), Calcul Québec and Compute Canada. SD is grateful for financial support through the McGill Engineering Doctoral Awards (MEDA). ADR is grateful for financial support through the James McGill Professorship appointment.

Data Availability

The raw data required to reproduce this manuscript findings cannot be shared at this time because the data are part of an ongoing study.

Discloser Statement

No conflict of interest.

References

[1] Sloan ED, Koh CA. Clathrate hydrates of natural gases. Boca Raton, FL: CRC Press; 2008.

[2] Carroll JJ. Natural gas hydrates: a guide for engineers. Waltham, Massachusetts: Gulf Professional Publishing; 2014.

[3] Barnes BC, Sum AK. Advances in molecular simulations of clathrate hydrates. Curr Opin Chem Eng. 2013;2(2):184-190.

[4] Ripmeester JA, John ST, Ratcliffe CI, et al. A new clathrate hydrate structure. Nature. 1987;325(6100):135-136.

[5] Sloan ED. Gas hydrates: review of physical/chemical properties. Energ Fuel. 1998;12(2):191-196.

[6] Pratt RM, Mei D-H, Guo T-M, et al. Structure H clathrate unit cell coordinates and simulation of the structure H crystal interface with water. J Chem Phys. 1997;106(10):4187-4195.

[7] Strobel TA, Koh CA, Sloan ED. Hydrogen storage properties of clathrate hydrate materials. Fluid Phase Equilibr. 2007;261(1-2):382-389.

[8] Veluswamy HP, Kumar R, Linga P. Hydrogen storage in clathrate hydrates: current state of the art and future directions. Appl Energ. 2014;122:112-132.

[9] Huo H, Liu Y, Zheng Z, et al. Mechanical and thermal properties of methane clathrate hydrates as an alternative energy resource. J Renew Sustain Ener. 2011;3(6):063110.

[10] Lederhos J, Mehta A, Nyberg G, et al. Structure H clathrate hydrate equilibria of methane and adamantane. AIChE J. 1992;38(7):1045-1048.

[11] Shin W, Park S, Koh D-Y, et al. Water-soluble structure H clathrate hydrate formers. J Phys Chem C. 2011;115(38):18885-18889.

[12] Susilo R, Lee J, Englezos P. Liquid–liquid equilibrium data of water with neohexane, methylcyclohexane, tert-butyl methyl ether, n-heptane and vapor–liquid–liquid equilibrium with methane. Fluid Phase Equilibr. 2005;231(1):20-26.

[13] Erfan-Niya H, Modarress H. Molecular dynamics simulation of structure H clathrate-hydrates of binary guest molecules. J Nat Gas Chem. 2011;20(6):577-584.

[14] Alavi S, Ripmeester J, Klug D. Stability of rare gas structure H clathrate hydrates. J Chem Phys. 2006;125(10):104501.

[15] Murayama K, Takeya S, Alavi S, et al. Anisotropic lattice expansion of structure H clathrate hydrates induced by help guest: experiments and molecular dynamics simulations. J Phys Chem C. 2014;118(37):21323-21330.

[16] Tse JS. Thermal expansion of structure-H clathrate hydrates. J Inclus Phenom Mol. 1990;8(1):25-32.

[17] Takeya S, Hori A, Uchida T, et al. Crystal lattice size and stability of type H clathrate hydrates with various large-molecule guest substances. J Phys Chem B. 2006;110(26):12943-12947.

[18] Ning F, Yu Y, Kjelstrup S, et al. Mechanical properties of clathrate hydrates: status and perspectives. Energ Environ Sci. 2012;5(5):6779-6795.

[19] Tezuka K, Murayama K, Takeya S, et al. Effect of guest size and conformation on crystal structure and stability of structure H clathrate hydrates: experimental and molecular dynamics simulation studies. J Phys Chem C. 2013;117(20):10473-10482.

[20] Hiratsuka M, Ohmura R, Sum AK, et al. Vibrational modes of methane in the structure H clathrate hydrate from ab initio molecular dynamics simulation. J Chem Phys. 2012;137(14):144306.

[21] Susilo R, Alavi S, Ripmeester JA, et al. Molecular dynamics study of structure H clathrate hydrates of methane and large guest molecules. J Chem Phys. 2008;128(19):194505.

[22] Imasato K, Murayama K, Takeya S, et al. Effect of nitrogen atom substitution in cyclic guests on properties of structure H clathrate hydrates. Can J Chem. 2015;93(8):906-912.

[23] Shu J, Chen X, Chou I-M, et al. Structural stability of methane hydrate at high pressures. Geosci Front. 2011;2(1):93-100.

[24] Ripmeester J, Ratcliffe C. Xenon-129 NMR studies of clathrate hydrates: new guests for structure II and structure H. J Phys Chem. 1990;94(25):8773-8776.

[25] Tsuji H, Ohmura R, Mori YH. Forming structure-H hydrates using water spraying in methane gas: effects of chemical species of large-molecule guest substances. Energ Fuel. 2004;18(2):418-424.

[26] Erfani A, Varaminian F. Experimental investigation on structure H hydrates formation kinetics: effects of surfactants on interfacial tension. J Mol Liq. 2017;225:636-644.

[27] Lenz A, Ojamäe L. Structures of the I-, II-and H-methane clathrates and the ice− methane clathrate phase transition from quantum-chemical modeling with force-field thermal corrections. The Journal of Physical Chemistry A. 2011;115(23):6169-6176.

[28] Inerbaev TM, Belosludov VR, Belosludov RV, et al. Theoretical study of clathrate hydrates with multiple occupation. J Incl Phenom Macro. 2004;48(1-2):55-60.

[29] Liu J, Yan Y, Chen G, et al. Prediction of efficient promoter molecules of sH hydrogen hydrate: an ab initio study. Chem Phys. 2019;516:15-21.

[30] Román-Pérez G, Moaied M, Soler JM, et al. Stability, adsorption, and diffusion of CH_4, CO_2, and H_2 in clathrate hydrates. Phys Rev Lett. 2010;105(14):145901.

[31] Vlasic TM, Servio P, Rey AD. Atomistic modeling of structure II gas hydrate mechanics: Compressibility and equations of state. AIP Adv. 2016;6(8):085317

[32] Khokhar A, Gudmundsson J, Sloan E. Gas storage in structure H hydrates. Fluid Phase Equilibr. 1998;150:383-392.

[33] Makino T, Nakamura T, Sugahara T, et al. Thermodynamic stability of structure-H hydrates of methylcyclopentane and cyclooctane helped by methane. Fluid Phase Equilibr. 2004;218(2):235-238.

[34] Giustino F. Materials modelling using density functional theory: properties and predictions. Oxford University Press; 2014.

[35] Humphrey W, Dalke A, Schulten K. VMD: visual molecular dynamics. J Mol Graphics. 1996;14(1):33-38.

[36] Soler JM, Artacho E, Gale JD, et al. The SIESTA method for ab initio order- N materials simulation. J Phys-Condens Mat. 2002;14(11):2745-2779.

[37] Zhang Y, Yang W. Comment on "generalized gradient approximation made simple". Phys Rev Lett. 1998;80(4):890-890.

[38] Jendi ZM, Rey AD, Servio P. Ab initio DFT study of structural and mechanical properties of methane and carbon dioxide hydrates. Mol Simulat. 2015;41(7):572-579.

[39] Dion M, Rydberg H, Schröder E, et al. Van der Waals density functional for general geometries. Phys Rev Lett. 2004;92(24):246401.

[40] Román-Pérez G, Soler JM. Efficient implementation of a van der Waals density functional: application to double-wall carbon nanotubes. Phys Rev Lett. 2009;103(9):096102.

[41] Okano Y, Yasuoka K. Free-energy calculation of structure-H hydrates. J Chem Phys. 2006;124(2):024510.

[42] Schaftenaar G, Noordik JH. Molden: a pre-and post-processing program for molecular and electronic structures. J Comput Aid Mol Des. 2000;14(2):123-134.

[43] Murnaghan F. The compressibility of media under extreme pressures. P Natl Acad Sci USA. 1944;30(9):244-247.

[44] Birch F. Finite elastic strain of cubic crystals. Phys Rev B. 1947;71(11):809.

[45] Vinet P, Ferrante J, Rose J, et al. Compressibility of solids. J Geophys Res-Sol Ea. 1987;92(B9):9319-9325.

[46] Patiño Douce A. Thermodynamics of the earth and planets. Cambridge: Cambridge University Press; 2011.

[47] Susilo R, Ripmeester JA, Englezos P. Characterization of gas hydrates with PXRD, DSC, NMR, and Raman spectroscopy. Chem Eng Sci. 2007;62(15):3930-3939.

[48] Jin Y, Kida M, Nagao J. Structural characterization of structure H (sH) clathrate hydrates enclosing nitrogen and 2,2-dimethylbutane. J Phys Chem C. 2015;119(17):9069-9075.

[49] Ohmura R, Uchida T, Takeya S, et al. Phase equilibrium for structure-H hydrates formed with methane and either pinacolone (3,3-dimethyl-2-butanone) or pinacolyl alcohol (3,3-dimethyl-2-butanol). J Chem Eng Data. 2003;48(5):1337-1340.

[50] Murayama K, Takeya S, Ohmura R. Phase equilibrium and crystallographic structure of clathrate hydrate formed in argon+2,2-dimethylbutane+water system. Fluid Phase Equilibr. 2014;365:64-67.

[51] Tulk CA, Machida S, Klug DD, et al. The structure of CO_2 hydrate between 0.7 and 1.0 GPa. J Chem Phys. 2014;141(17):174503.

[52] Yang L, Tulk CA, Klug DD, et al. Guest disorder and high pressure behavior of argon hydrates. Chem Phys Lett. 2010;485(1):104-109.

[53] Manakov AY, Likhacheva AY, Potemkin VA, et al. Compressibility of gas hydrates. Chemphyschem. 2011;12(13):2476-2484.

[54] Zele SR, Lee SY, Holder GD. A theory of lattice distortion in gas hydrates. J Phys Chem B. 1999;103(46):10250-10257.

[55] Xu B, Wang Q, Tian Y. Bulk modulus for polar covalent crystals. Sci Rep. 2013;3:3068-3068. PubMed PMID: 24166098.

[56] Jiang H, Jordan KD. Comparison of the properties of xenon, methane, and carbon dioxide hydrates from equilibrium and nonequilibrium molecular dynamics simulations. J Phys Chem C. 2010;114(12):5555-5564.

[57] Li Q, Kolb B, Román-Pérez G, et al. Ab initio energetics and kinetics study of H_2 and CH_4 in the SI clathrate hydrate. Phys Rev B. 2011;84(15):153103.

[58] Papadimitriou NI, Tsimpanogiannis IN, Papaioannou AT, et al. Monte Carlo study of sII and sH argon hydrates with multiple occupancy of cages Mol Simulat. 2008;34(10-15):1311-1320.

[59] Anderson BJ, Tester JW, Trout BL. Accurate potentials for argon−water and methane−water interactions via ab initio methods and their application to clathrate hydrates. J Phys Chem B. 2004;108(48):18705-18715.

[60] Liu J, Yan Y, Zhang J, et al. Theoretical investigation of storage capacity of hydrocarbon gas in sH hydrate. Chem Phys. 2019;525:110393.

[61] Anderson OL, Nafe JE. The bulk modulus-volume relationship for oxide compounds and related geophysical problems. J Geophys Res-Sol Ea. 1965;70(16):3951-3963.

[62] Tsubomura H. The nature of the hydrogen-bond. I. The delocalization energy in the hydrogen-bond as calculated by the atomic-orbital method. B Chem Soc JPN. 1954;27(7):445-450.

[63] Levitin V. Interatomic bonding in solids: fundamentals, simulation, applications. John Wiley & Sons; 2014.

[64] Gudkovskikh SV, Kirov MV. Proton disorder and elasticity of hexagonal ice and gas hydrates. J Mol Model. 2019;25(2):32.

[65] Vlasic TM, Servio PD, Rey AD. Effect of guest size on the mechanical properties and molecular structure of gas hydrates from first-principles. Cryst Growth Des. 2017;17(12):6407-6416.

[66] Gagnon R, Kiefte H, Clouter M, et al. Acoustic velocities and densities of polycrystalline ice Ih, II, III, V, and VI by Brillouin spectroscopy. J Chem Phys. 1990;92(3):1909-1914.

[67] Jendi ZM, Servio P, Rey AD. Ideal strength of methane hydrate and ice Ih from first-principles. Cryst Growth Des. 2015;15(11):5301-5309.